minerals

MDPI

Article

The Role of Chloride Ions during the Formation of Akaganéite Revisited

Johanna Scheck, Tobias Lemke and Denis Gebauer *

Received: 7 October 2015; Accepted: 17 November 2015; Published: 23 November 2015
Academic Editors: Karim Benzerara, Jennyfer Miot and Thibaud Coradin

Department of Chemistry, Physical Chemistry, University of Konstanz, Universitätsstr. 10, 78457 Konstanz, Germany; johanna.scheck@uni-konstanz.de (J.S.); tobias.lemke@uni-konstanz.de (T.L.)
* Correspondence: Denis.Gebauer@uni-konstanz.de; Tel.: +49-7531-882169; Fax: +49-7531-883139

Abstract: Iron(III) hydrolysis in the presence of chloride ions yields akaganéite, an iron oxyhydroxide mineral with a tunnel structure stabilized by the inclusion of chloride. Yet, the interactions of this anion with the iron oxyhydroxide precursors occurring during the hydrolysis process, as well as its mechanistic role during the formation of a solid phase are debated. Using a potentiometric titration assay in combination with a chloride ion-selective electrode, we have monitored the binding of chloride ions to nascent iron oxyhydroxides. Our results are consistent with earlier studies reporting that chloride ions bind to early occurring iron complexes. In addition, the data suggests that they are displaced with the onset of oxolation. Chloride ions in the akaganéite structure must be considered as remnants from the early stages of precipitation, as they do not influence the basic mechanism, or the kinetics of the hydrolysis reactions. The structure-directing role of chloride is based upon the early stages of the reaction. The presence of chloride in the tunnel-structure of akagenéite is due to a relatively strong binding to the earliest iron oxyhydroxide precursors, whereas it plays a rather passive role during the later stages of precipitation.

Keywords: akaganéite; iron(III) hydrolysis; iron oxide; ion-selective electrode measurements; titration assay

1. Introduction

The hydrolysis of iron(III) salts leads to a broad variety of iron(oxyhydr)oxides depending on many different parameters such as pH, temperature and the anion present in the reaction mixture [1–11]. These iron(oxyhydr)oxide species play an important role not only for numerous applications but also as crucial materials for living organisms in different habitats [1,12,13]. In biomineralization processes, bacterial cells produce a variety of iron minerals by precipitation, whereas the organisms control the structure of the forming solid using different strategies [1,14–18]. For example, the negatively charged cell walls of iron mineral producing bacteria can bind the iron cations. Nucleation and growth is then induced at the cell wall [14,18,19]. In these cases, the products of biomineralization resemble the precipitates that are found in purely inorganic environments and factors such as the presence of certain counter-ions determine which iron phase is formed [14]. Hence, understanding of inorganic mineralization is crucial for the understanding of the formation of minerals by bacteria. Besides the precipitation processes induced by bacteria, several organisms are known to transform iron (oxyhydr)oxides by oxidation or reduction reactions [1,13,15,16,20]. Typical precursor phases for the transformation into the mixed-valent magnetic iron oxides magnetite and maghemite are poorly crystalline phases such as ferrihydrite or akaganéite [17,20]. Akaganéite itself can be obtained by bioinduced mineralization [17].

In inorganic systems, the presence of chloride ions is known to play a directive role in the formation of akaganéite [1–3,5–8,21]. This mineral exhibits interesting properties due to its tunnel

structure, which can be exploited in different applications such as ion exchange or sorption [22–24]. While it is known that chloride ions are incorporated into the final structure of the product when being present during the hydrolysis of aqueous iron(III) solutions, the complicated reaction mechanisms of iron hydrolysis render a complete understanding of the directive properties of chloride ions difficult. There have been ongoing debates on fundamental questions concerning the reaction stage, at which the chloride ions direct the development towards akaganéite and get incorporated into the structure. It has been suggested that chloride ions react with the earliest species occurring during the hydrolysis reaction [25], and are then removed by hydrolysis from the growing colloidal species after being bound within mono- and dinuclear complexes [25,26]. Recent molecular dynamics simulations indeed show binding of chloride ions to mononuclear complexes, but they are released simultaneously already to the formation of polynuclear clusters [27]. In contrast to these studies, so-called akaganéite embryos have been suggested to form the final precipitate via aggregation [28,29]. These embryos are considered as early products of the hydrolysis with structures resembling the final crystal lattice. For the latter case, expulsion of chloride ions from the first coordination shell of iron(III) ions was detected at the very onset of hydrolysis.

In addition to the above examples, the mechanistic role of chloride ions during iron hydrolysis has been discussed frequently. Dousma *et al.* [25] described iron complexes with chloride ions in a bridging position for early, low molecular species. In this case, the hydrolysis reaction is promoted in the presence of chloride ligands, due to a decreased distance of the iron cores and an increased stability of the specific conformation, which facilitates the reaction [30]. This suggestion contradicts the picture, in which the chloride ion is merely a passive spectator and bridging by chloride is explicitly excluded, but instead plays a key role during later aggregation processes [26,27]. The presence of chloride in the hydrolyzed species was in this case attributed to an incomplete replacement by hydroxo- or oxo-ligands [26,28], which is essentially determined by the kinetics of the process.

Herein, we address these debated key questions regarding the influence of chloride during the early stages of iron(III) hydrolysis in aqueous systems. A titration assay with a chloride ion-selective electrode (ISE) was implemented to measure quantitatively the amount of free (*i.e.*, non-reacted) and bound chloride ions throughout homogenous, controlled hydrolysis experiments. This experimental setup enables a quantitative access to the distinct, early stages of the reaction. Chloride ISE measurements during iron(III) hydrolysis have not been reported previously, and complement the abovementioned studies. This enables us to contribute to the ongoing debate on the role of chloride during akagenéite formation.

2. Experimental Section

2.1. General

All chemicals were used as received: iron(III) chloride hexahydrate (Sigma Aldrich, St. Louis, MO, USA, purissimum pro analysi, ACS reagent, 98.0%–102%), hydrochloric acid (Merck, Kenilworth, NJ, USA, 0.1 M), sodium hydroxide (Merck, 0.1 M), sodium chloride (VWR, Radnor, PA, USA, 99.9%), sodium nitrate (Merck, 99.5%), iron(III)chloride nonahydrate (Sigma Aldrich, purissimum pro analysi, ACS reagent, ⩾98%), nitric acid (Sigma Aldrich, purissimum pro analysi, reagent ISO, reagent European Pharmacopoeia, ⩾65%). All solutions and dilutions were prepared with water of Milli-Q quality, generated with a Milli-Q Direct water purification system (Merck Millipore, Billerica, MA, USA).

2.2. Titrations

The hydrolysis of the iron(III) salts was performed utilizing an automated commercially available titration setup provided by Metrohm (Filderstadt, Germany). The titration device (836 Titrando), which operates two dosing units (800 Dosino) is controlled by a custom-made software

(Tiamo 2.3, Metrohm). The dosing units are equipped with burettes holding special valves that are designed to prevent diffusion and also allow dosing at minimal rates of 0.01 mL/min into the titration reservoir. The valves were frequently cleaned with 0.1 M HCl. For the hydrolysis, 25 mL of a 0.01 M HCl solution were adjusted to a desired pH value by the addition of 0.05 M NaOH solution. Iron(III) chloride was dissolved in 0.1 M HCl to yield an iron concentration of 0.1 M. This solution was dosed into the hydrochloric acid at a rate of 0.01 mL/min. During this addition, the pH-value of the solution was measured with a pH electrode (Metrohm, EtOH-Trode, 6.0269.100), which features an additional electrolyte reservoir shielding the inner electrolyte of the inbuilt reference electrode, and automatically kept constant by the addition of 0.05 M NaOH. The outer electrolyte of the pH electrode was replaced by 1 M KNO_3 as the diffusion of the typically used electrolyte KCl through the electrode membrane into the solution would lead to an increase of the chloride concentration. 3 M KCl was used as inner electrolyte solution owing to the requirements of the reference system. The electrolyte solutions were replaced prior to every measurement. The pH electrode was calibrated every week using standardized pH buffers (Mettler-Toledo, Giessen, Germany).

For the titrations with higher initial chloride concentration, 0.146 g NaCl was dissolved in the 25 mL hydrochloric acid, to which the iron(III) solution was added.

Replacement of chloride ions by nitrate was achieved by dissolving $Fe(NO_3)_3 \cdot 9H_2O$ in nitric acid and adding this solution to 0.01 M HNO_3.

Cl^--activities were measured with a solid-state ion-selective electrode (Metrohm, 6.0502.120). Calibration measurements of the ISE were carried out by titrating a solution of 0.3 M NaCl and 0.3 M $NaNO_3$ to 0.01 M HCl that was previously adjusted to the desired pH value, while this pH value was kept constant analogous to the titration experiments. For both investigated pH values, calibrations were performed separately to account for activity effects [31], whereas the ionic strength was adjusted as indicated above. Moderate continuous changes of the ionic strength during the actual experiments were taken into account, based on the extended Debye-Hückel theory. The starting values of the ISE signal at the beginning of each experiment slightly differed from the expected value of the (initially known) chloride concentration. To avoid a systematic error, the electrode intercept obtained from calibration was corrected to fit the starting concentration of each experiments. The minor respective corrections were all within the standard deviation of the main electrode intercept determined by averaging the complete data set of calibrations (N = 3 for each pH-value).

2.3. Isolation and Characterization of Precipitates

The solid products resulting from the titrations were isolated and characterized. Therefore, the titration at pH 2.5 (respectively pH 2.7 for SEM/EDX analyses) was interrupted after titration over night to obtain a sufficient amount of precipitate. As discussed below, for pH 2.0, no precipitate can be obtained. The reaction solution was transferred into thick-walled polyallomer centrifuge tubes (13 × 51 mm, Beckman Coulter, Brea, CA, USA) and centrifuged for one hour at 32,000 rpm utilizing a preparative ultracentrifuge (Beckman Coulter). The sediment was separated from the solution by decantation and subsequently dried in a vacuum oven at 35 °C. Freeze drying of the isolated samples yielded the same product (data not shown).

Powder X-ray diffraction (P-XRD) measurements were performed using an AXS D8 Advance diffractometer with a Göbelmirror PGM by Bruker (Billerica, MA, USA). The experiments were carried out with Cu K_α radiation at a scanning rate of 0.15 2θ/min and the diffractogram was background corrected to account for iron fluorescence.

A tabletop microscope TM 3000 from HITACHI (Tokyo, Japan) was used for scanning electron microscopy (SEM) images and EDX measurements of the samples.

3. Results and Discussion

3.1. Binding of Chloride Ions during the Early Stages of Hydrolysis

Titrations performed at two different pH values are shown in Figure 1. The graph displays the amount of base that is required to maintain a constant pH level, plotted *versus* the concentration of added chloride ions (which correlates with the addition of iron(III)). It can be directly seen that for pH 2.0, no hydrolysis occurs, while at pH 2.5, a significant, nonlinear consumption of hydroxide ions is observed, which asymptotically approaches a linear progression. This behavior is the direct consequence of the complex hydrolysis reactions occurring in aqueous iron(III) solutions above ca. pH 2.2, whereas the ligand exchange of aquo- and chloro-ligands by hydroxo-ligands is monitored throughout the reaction. This exchange results in the generation of protons, as hydroxo-ligands are only accessible from the self-dissociation of water molecules, which is minor at this pH level, and the remaining protons are neutralized by hydroxide titration so as to maintain a constant pH.

Iron(III) oxy(hydr)oxide formation is based on the hydrolysis, as it yields the precursors for two distinct mechanisms of bridging iron complexes, *i.e.*, olation and oxolation [32–34]. The linear increase in the hydroxide consumption during the very early stage of the reaction (asymptote in Figure 1a) shows that the ligand exchange yields iron(III) complexes that contain not more than one hydroxo-ligand per iron center. Quantitatively, one hydroxo-ligand is present only in 40% of all iron(III) complexes during the early stage of the experiment. This is also consistent with a maximum of one hydroxo-ligand per iron(III) ion for this early stage of the reaction. Bridging of the iron(III) complexes via hydroxo-ligands (olation) cannot be traced by the titration experiments, as no protons are generated or hydroxides consumed, and additional analyses are required to evidence or rule out the presence of any such polymeric species. This will be subject to other work. However, in any case, the deviation of the hydroxide consumption from the initially linear slope is due to an increasing amount of protons produced upon hydrolysis. Thus, it is evident that the reaction from this point on, *i.e.*, starting with the first deviation from linear behavior, produces species that exhibit an increasing hydroxo/iron(III) ratio (which is about 2.8 at the end of the experiment). These species start to differ significantly from the initial iron(III) complexes containing only one hydroxo-ligand per mononuclear iron(III) center (and any potentially existing olation polymers thereof). In principle, it can be (i) the production of mononuclear iron(III) complexes containing more than one hydroxo-ligand; and/or (ii) a change in the speciation of the bridges in polynuclear olation complexes that may already exist. In the latter scenario, oxolation—*i.e.*, the bridging of iron complexes via oxo-bridges—can occur via either (iia) the release of a proton from an existing olation bridge, or (iib) the condensation of two iron(III) centers, each of which contains one hydroxo-ligand, and may or may not be part of a polynuclear complex. While process (iib) leads to the release of a water molecule that cannot be seen in the titration, it initially requires the exchange of two hydroxo-ligands (as opposed to one for olation), and both principle changes in reaction from olation to oxolation (iia/b) will lead to an increasing production of protons, as observed experimentally. In this context it should be noted that reaction path (iib) is based on close contact of two iron(III) complexes containing hydroxide ligands, which applies to only 40% of the iron(III) ions with an all-over iron(III) concentration range below 2 mM in the linear regime of the titration. Thus, while we cannot categorically exclude any oxolation via mechanism (iib) during this early stage of hydrolysis, it is rather unlikely to occur to any significant extent in the linear regime of the titration curve.

The hydrolysis development can be contrasted with the measured concentration of free chloride ions at both pH-values (Figure 1b), shown together with the theoretical concentration given by all added chloride ions. The measurements at the two pH-values differ significantly from the theoretical values. At pH 2.0, 5% of the added chloride ions cannot be detected in the solution, as they are bound to the iron species, which, however, do not hydrolyze (Figure 1a). This gives a ratio of bound chloride ions, *i.e.*, chloro-ligands to iron(III) ions in the solution of about 0.25, indicating that on average, about a quarter of the iron complexes present in non-hydrolyzing solution contain chloro-ligands. At

pH 2.5, a change in the development of the free chloride concentration during the titration experiment is found.

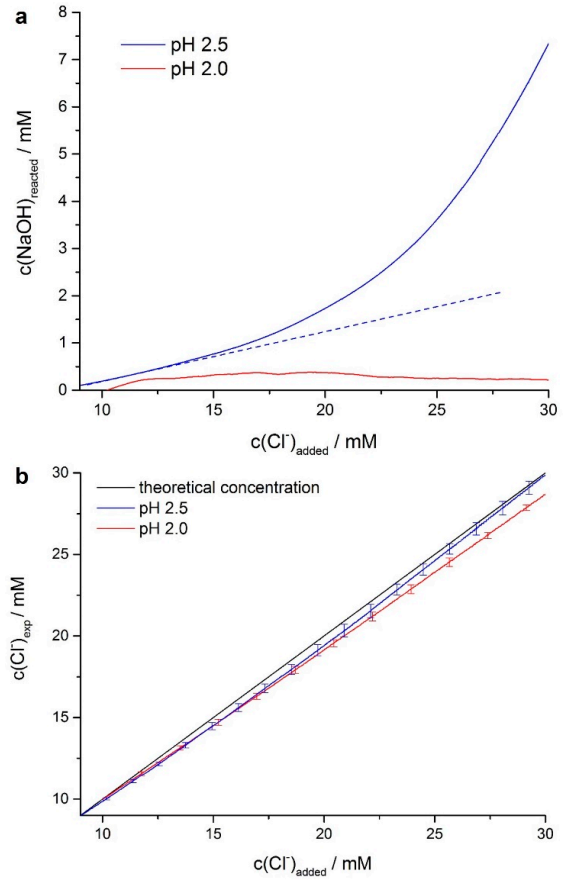

Figure 1. (**a**) Titration data showing the amount of hydroxide ions consumed in the hydrolysis reaction at pH 2.0 and 2.5 as indicated. The added asymptote (blue dashed line) is a guide for the eye to identify the change in hydrolysis as the first deviation from the initially linear progression. The graphs represent individual experiments; the reproducibility of the titration data is in general very good as can be seen in Figure 3; (**b**) Corresponding development of the concentration of free chloride ions in the solution from measurements with a chloride ion-selective electrode (ISE). The total added amount, giving the theoretical chloride concentration, is shown in black. The graphs for titrations at pH 2.0 (red) and 2.5 (blue) are averaged values from at least three individual titrations (error bars display +/− 1-σ-standard deviations).

The point at which the amount of bound chloride decreases coincides with the evident change in hydrolysis reaction discussed above, within experimental accuracy. Since iron(III) and chloride ions are continuously added, this leads to a decreasing Cl^{-}/Fe^{3+} ratio. The fact that the change in the free chloride concentration coincides with the change in the hydrolysis mechanism (Figure 1a) strongly suggests that this point correlates with the onset of oxalation. This is because our data shows that within experimental accuracy, the hydroxo-ligand exchange, which initially yields mononuclear iron(III) complexes containing a single hydroxo-ligand (or olation polymers thereof), does not result in any release of chloro-ligands within experimental accuracy (asymptote in Figure 1a when contrasted with Figure 1b). This suggests a similar binding for aquo- and hydroxo-ligands at the corresponding concentrations, and we argue that additional hydroxo-substitution at single iron(III) centers (mechanism (i) discussed above) cannot explain the onset of chloro-ligand release. The formation of oxo-bridges (mechanisms (iia) and (iib) discussed above), however, will bring about a much stronger and hence less dynamic iron-oxygen-bridging, and from the point of view of

ligand binding strengths, the observed release of chloro-ligands relates to the dehydration (release of aquo-ligands) upon condensation. This also confirms the findings of earlier studies, which claim that chloride ions are expelled from the nascent mineral with proceeding reaction [25–27]. In addition, our data strongly suggests that the chloride ions indeed remain in the complexes during all stages of hydrolysis, but that their partial expulsion begins with the onset of oxolation processes.

3.2. Chloride Content of the Formed Precipitates

Precipitates of titrations were isolated and characterized. Reflexes in the P-XRD diffraction pattern clearly evidence the presence of akaganéite as can be seen in Figure 2a (the corresponding reflexes are labeled by red diamonds). Drying effects from the isolation procedure cannot be excluded, but by different drying methods (vacuum, 35 °C and freeze-drying) akaganéite was obtained, indicating that drying effects play a minor role in this system, at least with respect to akagenéite formation. EDX analyses (Figure 2b) enable an estimation of the chloride to iron(III) ratio of 0.09 in the crystal structure. This is slightly higher than the reported chloride levels in akaganéite crystals, which typically range from 2 to 7 mol % [1]. However, it has to be noted that the value obtained here may be higher due to small amounts of NaCl in the sample. Nevertheless, the analyses confirm akaganéite formation with incorporation of chloride ions into the crystal lattice. When comparing this information to the titration experiments, our data indicate that the composition of the species present during hydrolysis change throughout the proceeding reaction, starting as complexes with a chloride to iron ratio of about 0.25, eventually resulting in akaganéite with a much lower ratio of about 0.09. This strongly indicates that the suggested akaganéite embryos [28,29] can only occur significantly after the onset of the oxolation processes. Earlier species contain distinctly more chloride, and therefore, very likely have a different structure than the final akaganéite phase.

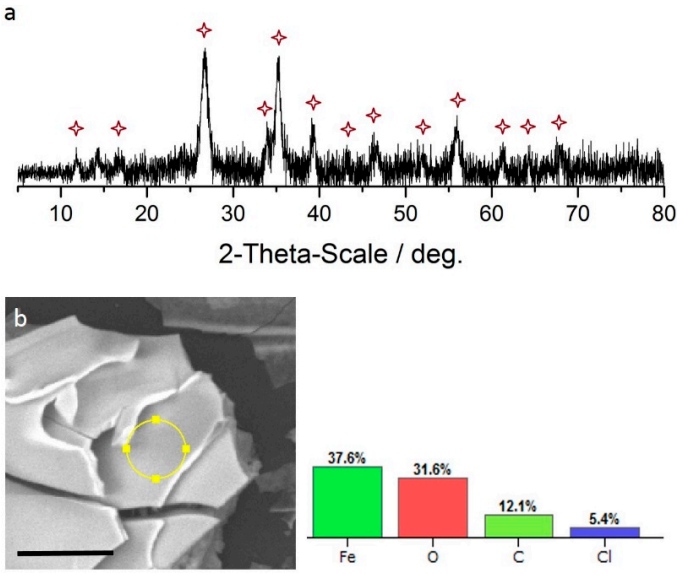

Figure 2. (**a**) Powder X-ray diffraction (P-XRD) scattering pattern of the isolated solid phase. The red labeled reflexes correspond to akaganéite; (**b**) **Left**: SEM image of the precipitate. The scale bar is 20 μm. **Right**: EDS result obtained from the region labeled with the yellow circle.

3.3. Influence of Chloride Ions on the Mechanism of Hydrolysis

The hydroxide consumption obtained from the titration data (see also Figure 1a) is a direct measure for the reaction rates, and can thus be used to identify any possible influence of chloride ions on the mechanism of hydrolysis. To that end, the titration experiment was carried out in the absence of chloride ions, where the $FeCl_3$ salt was replaced by $FeNO_3$, and instead of HCl, nitric

acid was used. In another comparative experiment, the total chloride concentration of the reaction solution was increased by the addition of 0.9 M NaCl to the starting solution. The titration data of the experiments with different chloride concentrations are shown in Figure 3. It has to be noted that the difference between the titration data shown in Figure 3a and b derives from the difference in pH and thus different hydroxide concentrations in the solution.

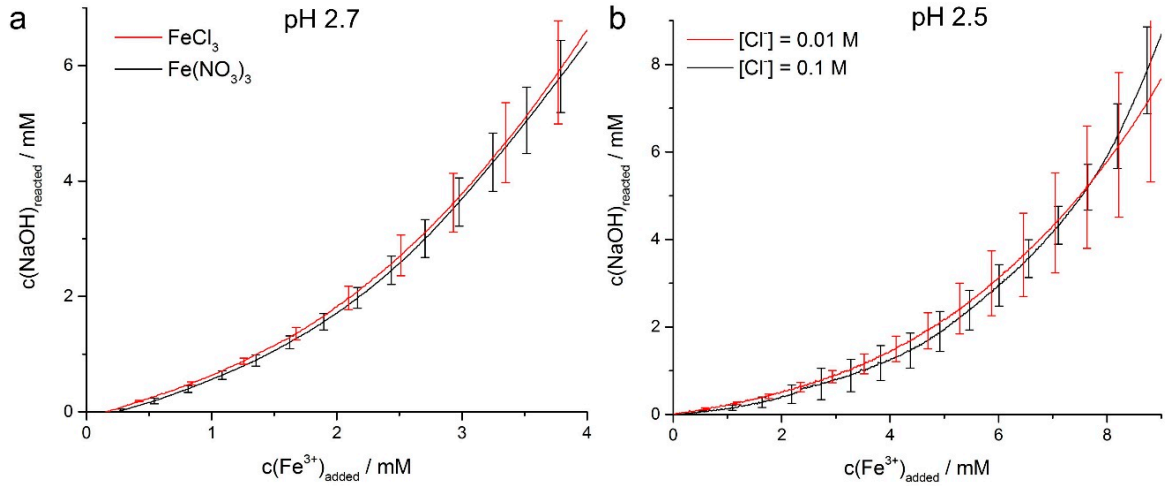

Figure 3. (**a**) Comparison of the hydrolysis of iron(III) chloride (red) and iron(III) nitrate (black). The titration was carried out at pH 2.7; (**b**) Titration data with different initial chloride concentrations at pH 2.5. The chloride concentration of the regular experiment of 0.01 M (red) was increased by the addition of NaCl to 0.1 M (black).

The data shows that the presence of the chloride ions has no influence on the reaction rate before and after the change in hydrolysis mechanism (arguably onset of oxolation), as the titration curves show the same behavior within the margin of error for all the investigated chloride concentrations. However, we cannot exclude any significant influence of the chloride ions at higher chloride- or iron(III)-concentrations. Nevertheless, the kinetics is not accelerated by an increased concentration of chloride ions in this concentration range, contradicting the results obtained by Dousma *et al.* [25]. In that work, different behavior for the consumption of base was observed depending on the presence and concentration of chloride ions, already in a much smaller range of Cl^{-}/Fe^{3+} ratios than investigated here. However, when compared to the titration experiments presented herein, the concentration of the solutions used and their mixing rates were significantly higher. This is problematic as homogeneous reaction conditions are crucial to examine the early stages of the reaction [8]. This implies that mixing artefacts may compromise the data of Dousma *et al.* [25].

4. Conclusions

This study shows that chloride ions actively bind to the earliest iron oxide precursors, but still play a rather passive role throughout the hydrolysis reaction of iron(III). The titration data evidence no influence on reaction rates, excluding any active chloride bridging of multinuclear iron complexes—as opposed to earlier studies [25]. With chloride in a bridging position, an earlier onset of oxolation, and with it, a change in kinetics of hydrolysis would be expected as the chloride concentration increases, which is not observed (Figure 3). For the non-hydrolyzing solution at pH 2.0, an equilibrium ratio of free chloride to iron(III) ions is maintained. The same binding is observed within experimental accuracy for the early stages of the hydrolysis at pH 2.5, indicating that mainly aquo-ligands are replaced by the added hydroxide, whereas the binding of aquo- and hydroxo-ligands is similar at the corresponding concentrations. As opposed to pH 2.0, however, the free chloride increases during the later stages of the reaction at higher pH (Figure 1). This confirms

not only that the chloride ions are displaced during the hydrolysis process; the data also strongly suggests that this process coincides with the onset of the oxolation reaction. After this event, the portion of bound chloride remains constant, and the iron(III) to chloride ratio decreases, as more and more iron(III) is hydrolyzed. This is very likely due to chloride ions being entrapped in the evolving more rigid (oxolated) iron oxyhydroxide structure, and these ions essentially end up as the chloride content in the final akaganéite mineral (Figure 2). It is intuitive that the final chloride content depends on the specific kinetics of the process, and heterogeneous mixing effects may account for the differing observations of Dousma *et al.* [25]. Moreover, as the composition of the earliest formed complexes significantly differs from that of the final solid, and expulsion of chloride ions towards the final crystal arguably takes only place after the onset of oxalation, akaganéite embryos [28,29] cannot occur before the onset of oxolation.

Taken together, the directive role of chloride ions towards the formation of akaganéite most likely arises from ordering processes within oxolated structures, which may be triggered by the aggregation of oxyhydroxide clusters (that contain the chloride). The cluster-based formation mechanism of iron oxyhydroxide is rather well established [32,33,35]. We speculate that the development of the tunnel structure of akagenéite is driven by the system's continuing drive to exclude chloride upon cluster aggregation and ongoing oxolation (*i.e.*, dehydration), which is thermodynamically preferred. However, it is kinetically hindered, if not impossible, owing to the rigidity of the aggregating oxolate clusters containing the chloride, and the chloride ions inside of an iron oxyhydroxide tunnel structure may be essentially conceived of as nanophase separation. From this point of view, the structure of akagenéite may be a compromise between the thermodynamics and kinetics of the process of iron hydrolysis in presence of chloride. Ultimately, the formation of akagenéite would be due to the thermodynamically preferable binding of chloride in the earliest iron oxyhydroxide precursors, as opposed to the final iron oxyhydroxide phases.

Acknowledgments: D.G. is a Research Fellow of the Zukunftskolleg of the University of Konstanz. We acknowledge support by the Fonds der Chemischen Industrie and the German Research Foundation (DFG) within project GE 2278/6-1, which is a part of the NSF-DFG "Materials World Network for Particle-mediated Control Over Crystallization: From the Pre-nucleation Stage to the Final Crystal". We thank Denise Castellanos for experimental assistance.

Author Contributions: D.G. and J.S. designed the research and wrote the manuscript. J.S. and T.L. carried out the experimental work.

Conflicts of Interest: The authors declare no conflict of interest.

References

1. Cornell, R.M.; Schwertmann, U. *The Iron Oxides*, 1st ed.; Wiley-VCH: Weinheim, Germany, 1997; pp. 488–495.
2. Blesa, M.A.; Matijevic, E. Phase transfomations of iron oxides, oxohydroxides, and hydrous oxides in aqueous media. *Adv. Colloid Interface Sci.* **1989**, *29*, 173–221. [CrossRef]
3. Murphy, P.J.; Posner, A.M.; Quirk, J.P. Characterization of partially neutralized ferric chloride solutions. *J. Colloid Interface Sci.* **1976**, *56*, 284–297. [CrossRef]
4. Murphy, P.J.; Posner, A.M.; Quirk, J.P. Characterization of partially neutralized ferric perchlorate solutions. *J. Colloid Interface Sci.* **1976**, *56*, 298–311. [CrossRef]
5. Murphy, P.J.; Posner, A.M.; Quirk, J.P. Characterization of hydrolyzed ferric ion solutions a comparison of the effect of various anions on the solutions. *J. Colloid Interface Sci.* **1976**, *56*, 312–319. [CrossRef]
6. Jolivet, J.P.; Chaneac, C.; Tronc, E. Iron oxide chemistry. From molecular clusters to extended solid networks. *Chem. Commun.* **2004**, *5*, 481–487. [CrossRef] [PubMed]
7. Flynn, C.M. Hydrolysis of inorganic iron(III) salts. *Chem. Rev.* **1984**, *84*, 31–41. [CrossRef]
8. Schneider, W. Hydrolysis of iron(III) . . . Chaotic olation *versus* nucleation. *Comments Inorg. Chem.* **1984**, *3*, 205–223. [CrossRef]
9. Schwertmann, U.; Friedl, J.; Pfab, G. A New Iron(III) Oxyhydroxynitrate. *J. Solid State Chem.* **1996**, *126*, 336. [CrossRef]

10. Schwertmann, U.; Friedl, J.; Stanjek, H. From Fe(III) Ions to Ferrihydrite and then to Hematite. *J. Colloid Interface Sci.* **1999**, *209*, 215–223. [CrossRef] [PubMed]
11. Hoffmann, A.; Vantelon, D.; Montargès-Pelletier, E.; Villain, F.; Gardoll, O.; Razafitianamaharavo, A.; Jaafar, G. Interaction of Fe(III) and Al(III) during hydroxylation by forced hydrolysis: The nature of Al–Fe oxyhydroxy co-precipitates. *J. Colloid Interface Sci.* **2013**, *407*, 76–88. [CrossRef] [PubMed]
12. Seder-Colomina, M.; Morin, G.; Benzerara, K.; Ona-Nguema, G.; Pernelle, J.-J.; Esposito, G.; van Hullebusch, E.D. *Sphaerotilus natans*, a Neutrophilic Iron-Related Sheath-Forming Bacterium: Perspectives for Metal Remediation Strategies. *Geomicrobiol. J.* **2014**, *31*, 64–75. [CrossRef]
13. Straub, K.L.; Benz, M.; Schink, B. Iron metabolism in anoxic environments at near neutral pH. *FEMS Microbiol. Ecol.* **2001**, *3*, 181–186. [CrossRef]
14. Konhauser, K.O. Diversity of bacterial iron mineralization. *Earth-Sci. Rev.* **1997**, *43*, 91–121. [CrossRef]
15. Faivre, D.; Godec, T.U. From Bacteria to Mollusks: The Principles Underlying the Biomineralization of Iron Oxide Materials. *Angew. Chem. Int. Ed.* **2015**, *54*, 4728–4747. [CrossRef] [PubMed]
16. Chan, C.; Fakra, S.C.; Edwards, D.C.; Emerson, D.; Banfield, J.F. Iron oxyhydroxide mineralization on microbial extracellular polysaccharides. *Geochim. Cosmochim. Acta* **2009**, *73*, 3807–3818. [CrossRef]
17. Brayner, R.; Yéprémian, C.; Djediat, C.; Coradin, T.; Herbst, F.; Livage, J.; Fiévet, F.; Couté, A. Photosynthetic Microorganism-Mediated Synthesis of Akaganeite (β-FeOOH) Nanorods. *Langmuir* **2009**, *25*, 10062–10067. [CrossRef] [PubMed]
18. Warren, L.; Ferris, F.G. Continuum between Sorption and Precipitation of Fe(III) on Microbial Surfaces. *Environ. Sci. Technol.* **1998**, *32*, 2331–2337. [CrossRef]
19. Bäuerlein, E. Biomineralization of Unicellular Organisms: An Unusual Membrane Biochemistry for the Production of Inorganic Nano- and Microstructures. *Angew. Chem. Int. Ed.* **2003**, *42*, 614–641. [CrossRef] [PubMed]
20. Lee, S.H.; Lee, I.; Roh, Y. Biomineralization of a poorly crystalline Fe(III) oxide, akaganeite, by an anaerobic Fe(III)-reducing bacterium (*Shewanella alga*) isolated from marine environment. *Geosci. J.* **2003**, *7*, 217–226. [CrossRef]
21. Atkinson, R.J.; Posner, A.M.; Quirk, J.P. Crystal nucleation and growth in hydrolysing iron(III) chloride solutions. *Clays Clay Miner.* **1977**, *25*, 49–56. [CrossRef]
22. Cai, J.; Liu, J.; Gao, Z.; Navrotsky, A.; Suib, S.L. Synthesis and anion exchange of tunnel structure akaganeite. *Chem. Mater.* **2001**, *15*, 4595–4602. [CrossRef]
23. Mazeina, L.; Deore, S.; Navrotsky, A. Energetics of bulk and nano-akaganeite, β-FeOOH: Enthalpy of formation, surface enthalpy, and enthalpy of water adsorption. *Chem. Mater.* **2006**, *18*, 1830–1838. [CrossRef]
24. Kolbe, F.; Weiss, H.; Morgenstern, P.; Wennrich, R.; Lorenz, W.; Schurk, K.; Stanjek, H.; Daus, B. Sorption of aqueous antimony and arsenic species onto akaganeite. *J. Colloid Interface Sci.* **2011**, *357*, 460–465. [CrossRef] [PubMed]
25. Dousma, J.; van den Hoven, T.J.; De Bruyn, P.L. The influence of chloride ions on the formation of iron(III) oxyhydroxide. *J. Inorg. Nucl. Chem.* **1977**, *40*, 1089–1093. [CrossRef]
26. Bottero, J.Y.; Manceau, A.; Villieras, F.; Tchoubar, D. Structure and mechanisms of formation of FeOOH(Cl) polymers. *Langmuir* **1994**, *10*, 316–319. [CrossRef]
27. Zhang, H.; Waychunas, G.A.; Banfield, J.F. Molecular dynamics simulation study of the early stages of nucleation of iron oxyhydroxide nanoparticles in aqueous solutions. *J. Phys. Chem. B* **2015**, *119*, 10630–10642. [CrossRef] [PubMed]
28. Combes, J.M.; Manceau, A.; Calas, G.; Bottero, J.Y. Formation of ferric oxides from aqueous solutions: A polyhedral approach by x-ray absorption spectroscopy: I. Hydrolysis and formation of ferric gels. *Geochim. Cosmochim. Acta* **1989**, *53*, 583–594. [CrossRef]
29. Manceau, A. Comment on "Direct observation of tetrahedrally coordinated Fe(III) in ferrihydrite". *Environ. Sci. Technol.* **2012**, *46*, 6882–6884. [CrossRef] [PubMed]
30. Brinker, C.J.; Scherer, W.G. *Sol-Gel Science: The Physics and Chemistry of Sol-Gel Processing*; Gulf Professional Publishing: Houston, TX, USA, 1990.
31. Kellermeier, M.; Picker, A.; Kempter, A.; Cölfen, H.; Gebauer, D. A straightforward treatment of activity in aqueous $CaCO_3$ solutions and the consequences for nucleation theory. *Adv. Mater.* **2014**, *26*, 752–757. [CrossRef] [PubMed]

32. Jolivet, J.-P.; Tronc, E.; Chanéac, C. Iron Oxides: From molecular clusters to solid. A nice example of chemical versatility. *Comptes Rendus Geosci.* **2006**, *338*, 488–497. [CrossRef]
33. Baumgartner, J.; Faivre, D. Iron solubility, colloids and their impact on iron(oxyhydr)oxide formation from solution. *Earth-Sci. Rev.* **2015**, *150*, 520–530. [CrossRef]
34. Brinker, C.J.; Scherer, W.G. *Sol-Gel Science: The Physics and Chemistry of Sol-Gel Processing*; Academic Press: Boston, MA, USA, 1990; pp. 22–30.
35. Gebauer, D.; Kellermeier, M.; Gale, J.D.; Bergström, L.; Cölfen, H. Pre-nucleation clusters as solute precursors in crystallization. *Chem. Soc. Rev.* **2014**, 2348–2371. [CrossRef] [PubMed]